



# Amphiphilic star block copolymers: Influence of branching on lyotropic/interfacial properties

Lei Wang, Ping Hu, Nicola Tirelli\*

School of Pharmacy and Pharmaceutical Sciences, University of Manchester, Oxford Road, Manchester, M13 9PT, United Kingdom

## ARTICLE INFO

### Article history:

Received 26 December 2008

Received in revised form

9 April 2009

Accepted 21 April 2009

Available online 3 May 2009

### Keywords:

Amphiphilic block copolymers

Star polymers

Lyotropic phases

## ABSTRACT

How can the degree of branching influence the lyotropic properties of amphiphilic block copolymers? In order to provide a qualitative answer to this question, we have prepared a library of poly(propylene sulfide)-*bl*-poly(ethylene glycol) (PPS-PEG) block copolymers, varying the hydrophobic block (PPS) length and its branching degree and thus producing diblock, triblock (that can be seen as two-armed star), tri-armed star and tetra-armed star structures. The PEG block, on the contrary, was kept constant (linear PEG2000).

Although all the polymers exhibited a qualitatively similar lyotropic behaviour, an increased degree of branching of the hydrophobic block caused clear differences in the rheology of lyotropic phases, with an increasingly softer character, and in the organisation of the PEG chains, which appeared to adopt possibly more extended and dehydrated conformations.

Crown Copyright © 2009 Published by Elsevier Ltd. All rights reserved.

## 1. Introduction

The use of block copolymers is probably the most travelled (and most effective) road that modern polymer chemistry offers for controlling the interfacial properties of materials. The “schizophrenic” nature of the polymers composed of incompatible blocks, e.g. hydrophilic and hydrophobic, opens the way to a variety of self-assembled morphologies, whose study has become increasingly popular with the development of versatile living/controlled polymerisation mechanisms (TEMPO-mediated, ATRP, RAFT).

Among the most noticeable results, it is worth mentioning the development of nano-structures, such as micelles [1] or vesicles [2], which, when produced by amphiphilic block copolymers as opposed to low MW amphiphilics, show much higher stability (mechanical, against dilution) and a better control over the interactions/response with external agents, such as biological factors or (combined) physico-chemical stimuli [3,4].

It is not our aim to provide a comprehensive overview of this vast and complex field, which can be obtained elsewhere [4–7]. We would rather draw the reader’s attention to the fact that the overwhelming majority of the studies related to the solvent-induced (lyotropic) aggregation behaviour of block copolymers

has focused on linear structures. For branched architectures, synthetic efforts [8–13] and physico-chemical studies of the behaviour in organic media [14,15] or in water [9,16,17] have mostly tackled macromolecules with a fixed degree of branching. Among the most noticeable studies where the influence of the branching degree was taken into account, one can mention those related to amphiphilic heteroarm star polymers, where both hydrophilic and hydrophobic chains converge towards the junction point [18–20].

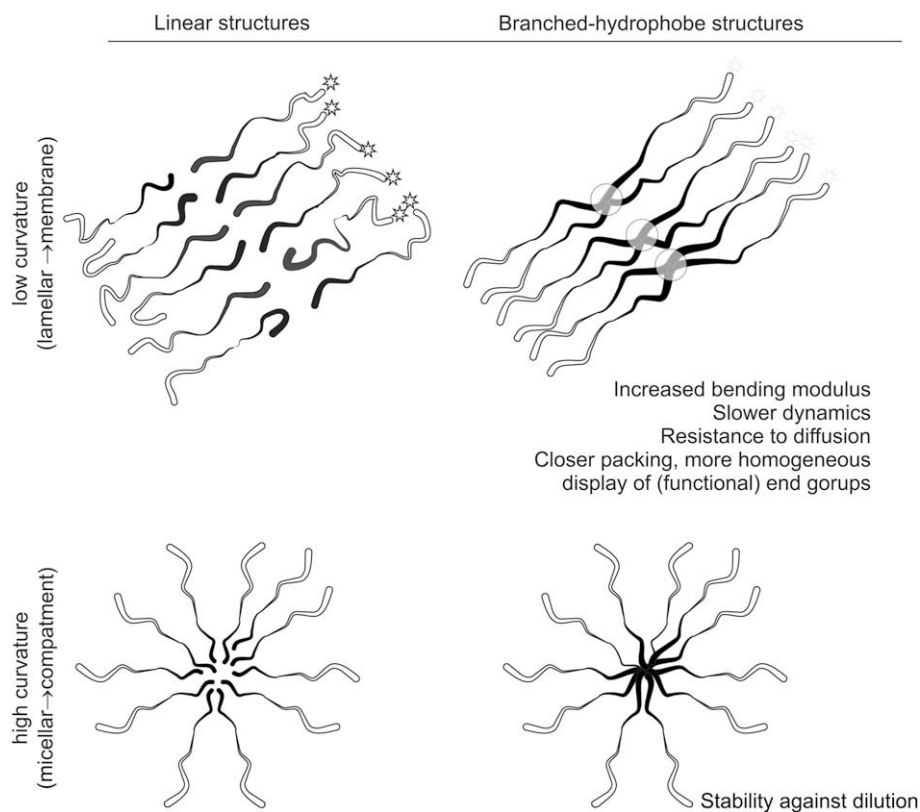
We are, on the contrary, specifically interested in understanding the influence that branching may have in one or the other block of an amphiphilic polymer. As an example, we may take poly(ethylene glycol) (PEG) as the hydrophilic block, whose linear amphiphilic block copolymers have been widely studied in biological environments. Branching in the hydrophobic domain could influence membrane properties in polymeric vesicles (larger bending elastic modulus, lower diffusion coefficients through the membrane) or the stability against dilution in micelles (branching would increase the tendency to form monomolecular micelles), but the hydrophobic branching can influence the PEG conformation and thus the distance between end-groups (→ clustering of ligands) or the protein repulsion of the nano-structure (Scheme 1).

In this paper we have started tackling these issues, trying to provide a qualitative assessment of the influence of branching on the lyotropic organisation PEG amphiphilic block copolymers by the use of a library of architectures with linear or star structure.

Abbreviations: PS, Propylene sulfide; TEA, Triethylamine; DBU, 1,8-Diazabicyclo undec-7-ene; TBP, Tributyl phosphine.

\* Corresponding author. Tel.: +44 161 275 24 80; fax: +44 161 275 23 96.

E-mail address: [nicola.tirelli@manchester.ac.uk](mailto:nicola.tirelli@manchester.ac.uk) (N. Tirelli).



**Scheme 1.** Possible effects of branching in the hydrophobic portion of self-assemblable amphiphilic block copolymers.

Specifically, we have utilised poly(propylene sulfide) (PPS) as a hydrophobic block. This macromolecular structure offers both synthetic versatility (anionic living polymerisation not sensitive to the presence of most protic compounds, including water [21]) and environmental responsiveness: the oxidation of the hydrophobic PPS leads to the production of hydrophilic polymers and this has opened the way to the production of a variety of oxidation-responsive nanomaterials [22–24], which may find application also in the targeting of inflammatory reactions [25,26].

Using methods originally developed for the synthesis of linear polymers [27] and then applied to that of star derivatives too [16], we have prepared a library of polysulfide block copolymers using initiators with variable functionality (1 to 4 thiol-equivalent groups) and different polysulfide/PEG ratios, in order to produce polymers with different branching degrees and hydrophilic/lipophilic balance. Specifically, depending on the structure of the initiator, linear diblock, linear triblock (2-armed star), 3-armed star and 4-armed star structures were produced, with polysulfide degree of polymerisation ranging from 10 to 40, while keeping constant PEG's degree of polymerisation to 44. This range of hydrophobic/hydrophilic balances was chosen, also on the basis of previous results [28], to ensure the formation of self-assembled structures with positive or at most zero curvature (e.g. micelles or lamellae/vesicles).

The above polymers have been studied in a water environment, either in concentrated polymer/water mixtures (rheology, polarised optical microscopy), or at the air–water interface (surface pressure/surface area isotherms), with the aim to highlight trends that (a) could be ascribed to differences in branching as opposed to differences in hydrophobic/hydrophilic balance and (b) could be attributed to a branching-dependent organisation of the hydrophobic or of the hydrophilic component.

## 2. Experimental section

### 2.1. Materials

All materials were used as received from the supplier (Aldrich, Gillingham, United Kingdom, for acetic acid, acetyl chloride, allyl bromide, allyl ethyl ether, diallyl ether, ethyl bromoacetate, molecular sieves, pentaerythritol allyl ether, poly(ethylene glycol) methyl ether ( $M_n = 2000$  g/mol), propylene sulfide, sodium hydride, thioacetic acid, triethylamine, 1,1,1-tris(hydroxymethyl)ethane, 2,2'-(ethylenedioxy) diethanethiol, 1,3-dimercaptopropane; Fluka, Gillingham, United Kingdom, for bromoacetyl bromide, Dowex resin, sodium methoxide solution, sodium methoxide, 1,8-diazabicyclo [5.4.0] undec-7-ene (1,5-5) (DBU), 4,4'-azobis (4-cyanovaleric acid)). THF was degassed by bubbling argon under inert atmosphere for 1 h before use.

### 2.2. Physico-chemical characterisation

#### 2.2.1. Molecular characterisation

$^1\text{H}$  NMR spectra were recorded on 1 wt.% polymer solutions in deuterated chloroform using a 500 MHz Bruker spectrometer. FT-IR spectra were recorded in ATR mode (Golden gate) on a Tensor 27 Bruker spectrometer. GPC was performed in THF on a Polymer Laboratories GPC 50 equipped with refractive index and viscosity detectors, using universal calibration with poly(styrene) standards.

#### 2.2.2. Polarised light optical microscopy

Copolymer films were prepared from dichloromethane solutions and water was added at different weight ratios (1:10, 2:10.4:10, 6:10, 10:10) and left in an incubator at room temperature for at least 72 h. Samples for the POM were prepared by applying the polymer/water mixtures on microscope slides, and sealing the

cover glasses with UHV grease (nail oil) to prevent water evaporation. The temperature-dependent polarised light optical micrographs were taken with the Leica DM 2500M microscope equipped with a hot stage (Mettler Toledo FP82HT) controlled by central processor unit (Mettler Toledo FP90) at heating rate of 1 °C/min.

### 2.2.3. Rheometry

The viscoelastic behaviour of the copolymer/water mixtures in the temperature range of 10–90 °C was studied by performing small-strain oscillatory shear experiments with a Bohlin CVO 120 rheometer using parallel plate geometry. Copolymer water mixtures were applied to the bottom plate and spread with a spatula. The upper plate (2 cm in diameter) was then immediately lowered to a measuring gap size of 0.10 mm. After 1 min of pre-shear at 1 Hz, the dynamic oscillating measurement, following the evolution of the storage ( $G'$ ) and loss ( $G''$ ) moduli at a frequency of 1 Hz, a stress of 1 Pa and at heating rate of 1 °C/min.

### 2.2.4. Langmuir balance surface area/pressure isotherms

100 mL of copolymer dichloromethane solutions ( $6.9 \times 10^{-5}$  M) were applied on the water surface on a Lauda FW 2 langmuir balance filled with double distilled water. After a period of at least 15 min, the surface area/pressure isotherm was recorded with a compression velocity of 50 cm<sup>2</sup>/min. The temperature was kept constant at 25 °C throughout all the phases of the process.

### 2.2.5. Preparative procedures

The block copolymers were prepared employing a literature procedure based on the use of protected thiols (in form of thioacetates), which are deprotected *in situ* via methanolysis with sodium methoxide and used to initiate the polymerisation of propylene sulfide. At the end of the polymerisation, the thiolate-terminated polymers are reacted with a PEG chain bearing a thiol-reactive 2-bromoacetate terminal group.

The initiators used in this study were *S*-(3-ethoxypropyl) ethane-thioate, *S,S'*-[ethane-1,2-diylbis (oxyethane-2,1-diyl)] diethanethioate, 1,1,1-tris(methanol (3-thioacetyl)propane ether)ethane, pentaerythritol tetrakis(3-thioacetyl propane), respectively, for the preparation of linear diblock, linear triblock, star tri-armed and star tetra-armed polymers. The synthesis of these initiators and of poly(ethylene glycol)  $\alpha$ -methyl ether- $\omega$ -2-bromoacetate is described in a previous publication [16].

### 2.2.6. Synthesis of linear and star shaped PPS-PEG block copolymers

A literature procedure based on the use of a reducing agent (TBP) during the polymerisation and of a buffer containing non-nucleophilic base in the end-capping step was adopted [29]. In a typical experiment, the polymerisation environment (parallel reactor FirstMate from Argonaut Technologies) was purged with argon for 5 min before polymerisation and 5 mL of previously degassed THF were introduced in each reactor. 1 mL of a thioacetate-containing compound stock solution in degassed THF (always corresponding to an amount of e.g. 64.8 mg/0.4 mmol of monofunctional initiator for mono PPS-PEG polymers or 60 mg/0.1 mmol of tetrafunctional initiator for tetraPPS-PEG polymers) and 1 mL of a TBP stock solution (corresponding to a 5-fold TBP: thioacetate group excess) was introduced in the reactor. A 1.05 equiv of sodium methanoate (0.5 M in methanol) was then added via a syringe, and the mixture was stirred at room temperature for 5 min. To the mixture was added a variable quantity (e.g. 20, 27, 40 or 80 equiv compared to thioacetate groups) of PS, and the reagents were allowed to react for 45 min. 1.1 equiv of acetic acid and 1.15 equiv of DBU were added to neutralise the pH. An excess of end-capping agent (2 equiv of poly(ethylene glycol)

$\alpha$ -methyl ether  $\omega$ -2-bromoacetate) was finally added, and the mixture was stirred for 2 h at room temperature.

The solvent was then removed, and the resulting viscous liquids were twice extracted with methanol, before being transferred to water and purified through ultrafiltration using membranes with MWCO = 30,000 g/mol; average yields after freeze drying = 65–80%.

All the homopolymers or block copolymers presented identical IR spectra, while clear differences are present in the NMR spectra depending on the kind of initiator used.

**FT-IR** (film on ATR crystal): **2956** ( $n_s$  CH<sub>3</sub>), **2886** ( $n_{as}$  CH<sub>2</sub>), **2861** ( $n_{as}$  CH<sub>3</sub> and  $n_s$  CH<sub>2</sub>), **1738** ( $n$  C=O ester), **1451** ( $\delta_s$  CH<sub>2</sub>), **1344**, **1280**, **1240**, **1145**, **1100** ( $n_{as}$  C–O–C), **960**, **844** ( $n_s$  C–O–C) cm<sup>-1</sup>. (in italics and underlined the absorptions that are largely increased by the presence of PEG, in bold those characteristic of the PPS chain).

**<sup>1</sup>H NMR** (CDCl<sub>3</sub>): **MonoPPS<sub>n</sub>-PEG<sub>44</sub>**:  $\delta$  = 1.15–1.20 (t, 3H, CH<sub>3</sub>CH<sub>2</sub>OCH<sub>2</sub>CH<sub>2</sub>CH<sub>2</sub>S–), 1.35–1.45 (d, CH<sub>3</sub> in PPS chain), 1.80–1.88 (q, 2H, CH<sub>3</sub>CH<sub>2</sub>OCH<sub>2</sub>CH<sub>2</sub>CH<sub>2</sub>S–), 2.55–2.75 (m, 1 diastereotopic H of CH<sub>2</sub> in PPS chain), 2.85–3.05 (m, CH and 1 diastereotopic H of CH<sub>2</sub> in PPS chain), 3.40 (s, 3H, –OCH<sub>3</sub>), 3.43–3.53 (t, 4H, CH<sub>3</sub>CH<sub>2</sub>OCH<sub>2</sub>CH<sub>2</sub>CH<sub>2</sub>S–), 3.6–3.8 (broad, PEG chain protons), 4.25–4.35 (m, 2H, OCH<sub>2</sub>CH<sub>2</sub>–O(O)C–) ppm.

**DiPPS-PEG**:  $\delta$  = 1.35–1.45 (d, CH<sub>3</sub> in PPS chain), 2.55–2.75 (m, 1 diastereotopic H of CH<sub>2</sub> in PPS chain), 2.71–2.78 (t, 4H, –SCH<sub>2</sub>CH<sub>2</sub>OCH<sub>2</sub>CH<sub>2</sub>OCH<sub>2</sub>CH<sub>2</sub>S–), 2.85–3.05 (m, CH and 1 diastereotopic H of CH<sub>2</sub> in PPS chain), 3.40 (s, 6H, –OCH<sub>3</sub>), 3.51–3.60 (t, 8H, –SCH<sub>2</sub>CH<sub>2</sub>OCH<sub>2</sub>CH<sub>2</sub>OCH<sub>2</sub>CH<sub>2</sub>S–), 3.6–3.8 (broad, PEG chain protons), 4.25–4.35 (m OCH<sub>2</sub>CH<sub>2</sub>–O(O)C–) ppm.

**TriPPS-PEG**:  $\delta$  = 0.90–0.93 (s, 3H, CH<sub>3</sub>C(CH<sub>2</sub>OCH<sub>2</sub>CH<sub>2</sub>CH<sub>2</sub>S–)<sub>3</sub>), 1.35–1.45 (d, CH<sub>3</sub> in PPS chain), 1.78–1.86 (q, 6H, CH<sub>3</sub>C(CH<sub>2</sub>OCH<sub>2</sub>CH<sub>2</sub>CH<sub>2</sub>S–)<sub>3</sub>), 2.55–2.75 (m, 1 diastereotopic H of CH<sub>2</sub> in PPS chain), 2.85–3.05 (m, CH and 1 diastereotopic H of CH<sub>2</sub> in PPS chain), 3.22–3.25 (s, 6H, CH<sub>3</sub>C(CH<sub>2</sub>OCH<sub>2</sub>CH<sub>2</sub>CH<sub>2</sub>S–)<sub>3</sub>), 3.40 (s, 9H, –OCH<sub>3</sub>), 3.53–3.56 (t, 6H, CH<sub>3</sub>C(CH<sub>2</sub>OCH<sub>2</sub>CH<sub>2</sub>CH<sub>2</sub>S–)<sub>3</sub>), 3.6–3.8 (broad, PEG chain protons), 4.25–4.35 (m, 6H, OCH<sub>2</sub>CH<sub>2</sub>–O(O)C–) ppm.

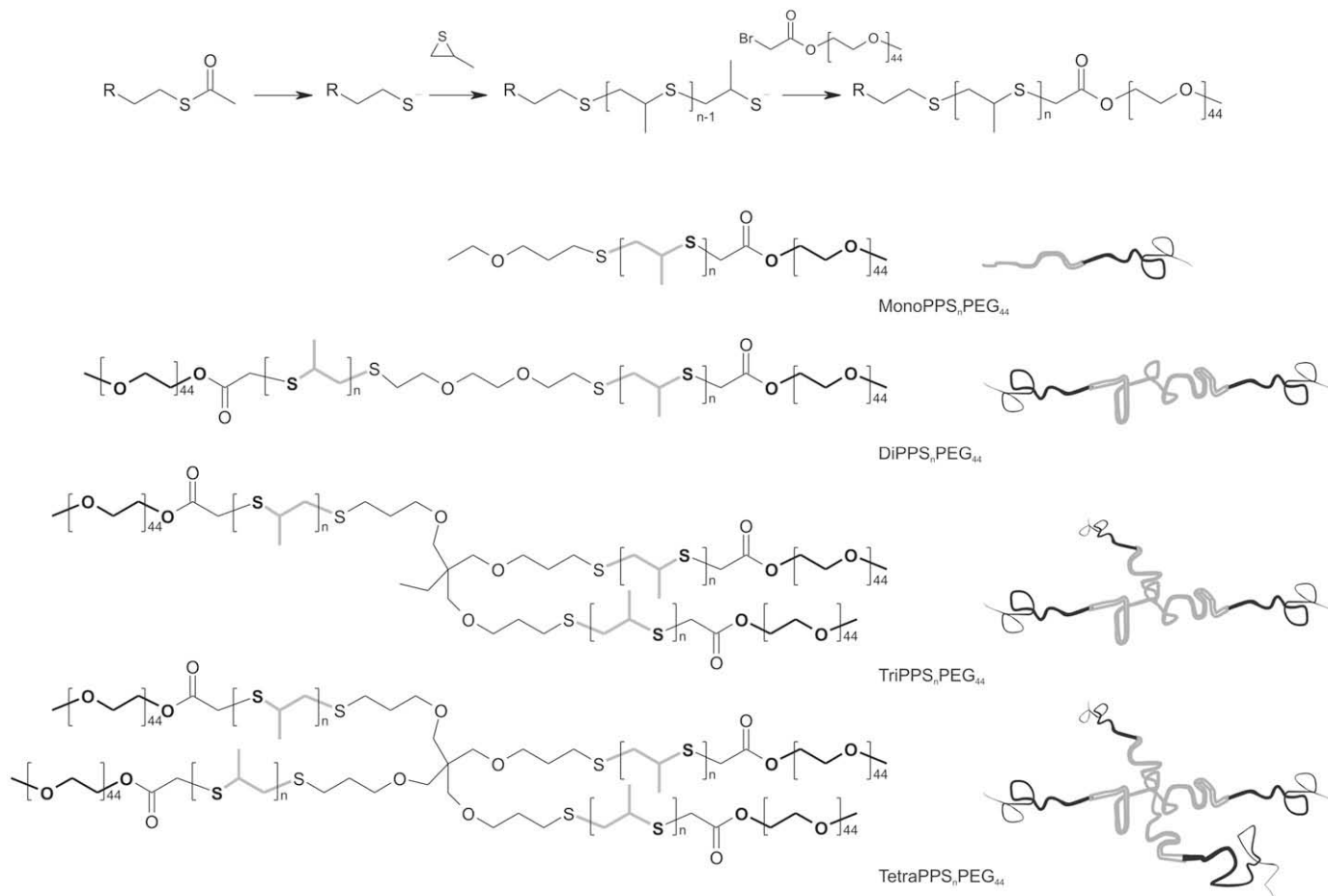
**TePPS-PEG**:  $\delta$  = 1.35–1.45 (d, CH<sub>3</sub> in PPS chain), 1.78–1.86 (q, 8H, –CH<sub>2</sub>OCH<sub>2</sub>CH<sub>2</sub>CH<sub>2</sub>S–), 2.55–2.75 (m, 1 diastereotopic H of CH<sub>2</sub> in PPS chain), 2.85–3.05 (m, CH and 1 diastereotopic H of CH<sub>2</sub> in PPS chain), 3.40 (s, 3H, –OCH<sub>3</sub>), 3.52–3.55 (s, 8H, –CH<sub>2</sub>OCH<sub>2</sub>CH<sub>2</sub>CH<sub>2</sub>S–), 3.56–3.61 (t, 8H, –CH<sub>2</sub>OCH<sub>2</sub>CH<sub>2</sub>CH<sub>2</sub>S–), 3.63–3.83 (broad, PEG chain protons), 4.25–4.35 (m, 8H, OCH<sub>2</sub>CH<sub>2</sub>–O(O)C–) ppm.

Please note that the signal of the methylene between terminal sulphur atoms of the PPS chain and carboxylic group of the PEG acetate falls between 3.2 and 3.3 ppm; however, it is broadened and difficult to measure in a quantitative fashion.

## 3. Results and discussion

### 3.1. Polymer synthesis and molecular characterisation

A sketch of the synthetic procedure is presented in Scheme 2, while the details of all polymers produced are provided in Table 1. The polydispersity index of the block copolymers and the end-capping yield are, respectively, always  $\leq 1.35$  and  $\geq 85\%$ , indicating that all polymer structures are reasonably well defined; however, the polydispersity increased and the end-capping yield decreased with increasing degree of branching, and, to a lesser extent, with increasing length of the polysulfide chain; this parallel behaviour suggests that a broader molecular weight dispersions stems from a less efficient introduction of PEG chains. We ascribe the dependence on the branching degree to the formation of intramolecular disulfide bonds, which would decrease the number of reactive groups: our previous experience has showed that disulfides are indeed very difficult to completely avoid also in the preparation of



**Scheme 2.** Initiators containing a variable number (1–4) of thiolates were produced *in situ* from the corresponding thioacetates and were subsequently used to polymerise propylene sulfide. The detailed description of the optimised synthetic procedure is presented elsewhere [29]. The resulting thiolate-terminated macromolecules were then end-capped with PEG bromoacetate.

linear polymers and this problem can be clearly worsened in a branched structure due to the local increased concentration of thiols. The dependence on the polymer length, on the contrary, can be due to the increasing steric hindrance on terminal groups of larger macromolecules.

In a previous paper we have shown that the intrinsic viscosity of linear or star low MW poly(propylene sulfide) samples does not appear to be influenced by the degree of branching; these data are reported in Fig. 1 as a reference. A numerical measure of the effect of branching can be obtained by calculating a contraction factor  $g_{\eta}$  from

**Table 1**  
Summary of the characteristics data for linear and star PPS-PEG samples.

Sample	End-capping yield (% mol) <sup>a</sup>	Overall yield (wt.%) <sup>b</sup>	No. of arms	Theor. DP of each PPS arm <sup>c</sup>	NMR $\overline{M}_n^d$	GPC <sup>e</sup> $M_n$	$\overline{M}_w/\overline{M}_n$	[ $\eta$ ](dL/g)
MonoPPS <sub>10</sub> PEG <sub>44</sub>	95%	72%	1	10	2800	3000	1.15	0.061
MonoPPS <sub>20</sub> PEG <sub>44</sub>	93%	70%	1	20	3400	3600	1.19	0.066
MonoPPS <sub>30</sub> PEG <sub>44</sub>	94%	73%	1	30	4400	4100	1.21	0.073
MonoPPS <sub>40</sub> PEG <sub>44</sub>	93%	75%	1	40	5200	5900	1.25	0.074
DiPPS <sub>10</sub> PEG <sub>44</sub>	91%	70%	2	10	5300	5600	1.21	0.076
DiPPS <sub>20</sub> PEG <sub>44</sub>	90%	72%	2	20	7100	7700	1.23	0.078
DiPPS <sub>30</sub> PEG <sub>44</sub>	92%	74%	2	30	8700	8100	1.26	0.087
DiPPS <sub>40</sub> PEG <sub>44</sub>	90%	76%	2	40	10200	10000	1.28	0.094
TriPPS <sub>10</sub> PEG <sub>44</sub>	90%	77%	3	10	8500	9000	1.23	0.107
TriPPS <sub>20</sub> PEG <sub>44</sub>	89%	73%	3	20	10900	11000	1.28	0.088
TriPPS <sub>30</sub> PEG <sub>44</sub>	88%	71%	3	30	12400	13600	1.30	0.092
TriPPS <sub>40</sub> PEG <sub>44</sub>	90%	77%	3	40	14500	16000	1.32	0.133
TetraPPS <sub>10</sub> PEG <sub>44</sub>	87%	68%	4	10	11600	11200	1.29	0.089
TetraPPS <sub>20</sub> PEG <sub>44</sub>	86%	70%	4	20	13600	15200	1.32	0.103
TetraPPS <sub>30</sub> PEG <sub>44</sub>	85%	65%	4	30	16000	16500	1.34	0.108
TetraPPS <sub>40</sub> PEG <sub>44</sub>	85%	66%	4	40	20700	19500	1.35	0.110

<sup>a</sup> From the ratio of the <sup>1</sup>H NMR signal of the PEG terminal CH<sub>3</sub> group and signals of the initiator.

<sup>b</sup> Weight of recovered polymer/weight of monomer + deprotected initiator + reacted PEG.

<sup>c</sup> Expressed as the ratio [PS]/[thiol].

<sup>d</sup> From the ratio of the <sup>1</sup>H NMR signal of the PPS CH<sub>3</sub> group in the terminal ester and the signals in the initiator structure.

<sup>e</sup> Calculated by the means of the universal calibration.



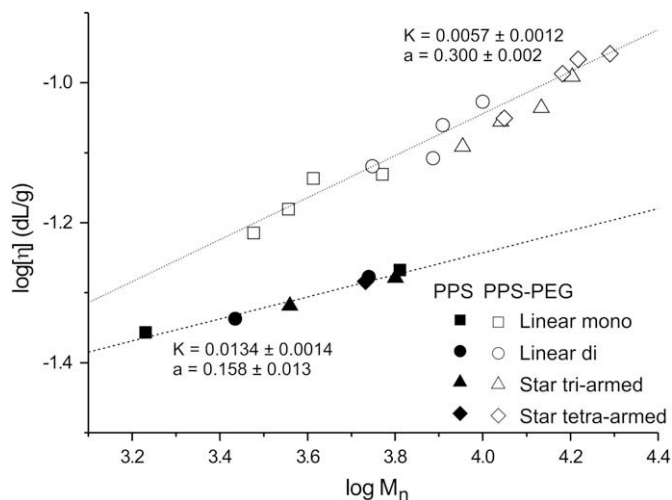


**Fig. 1.** log-log plot of intrinsic viscosity (in THF) vs. number average molecular weight for PPS-PEG block copolymers (empty symbols) and PPS homopolymers (black symbols). "Linear mono" and "linear di" stand for polymers produced from mono- and difunctional initiators, respectively.

the ratio of the intrinsic viscosities of polymers with the same molecular weight and composition but different degrees of branching. This ratio provides analogous information to the more common contraction factor  $g$  based on the square radii of gyration, since  $g_\eta = [\eta]_{\text{branched}}/[\eta]_{\text{linear}} = (R_{g-\text{branched}}^2/R_{g-\text{linear}}^2)^{2/3} = g^{2/3}$ . The contraction factors of for tri-armed star and tetra-armed star PPS homopolymers with  $\overline{M}_n \approx 6000$  g/mol are indeed equal to 1, within the experimental error, indicating that the presence of one branching point with functionality two or three was not sufficient to produce any significant contraction in the macromolecular coil dimension.

The same result is evident from the analysis of the intrinsic viscosity data (THF solution) for the PPS-PEG copolymers (Fig. 1) prepared in this study, with  $\log[\eta]$  exhibiting a linear relationship with  $\log(MW)$  independently on the nature of the block copolymer.

Due to this linearity, it is possible to fit the data with the Mark-Houwink equation, which allows to gather additional information on the macromolecular organisation in solution through its parameter  $a$ . PPS in THF solution shows  $a = 0.15$ , while PPS-PEG copolymers (constant PEG length) show  $a = 0.30$ , which is intermediate between that of PPS and the literature values for PEG ( $a = 0.66$  at  $T = 25^\circ\text{C}$  in THF [30]). It is well known that values  $>0.5$  indicate the polymer to be in a thermodynamically good solvent, while  $a < 0.5$  signals a poor solvent [31]. The above data therefore seem to indicate PPS to be significantly contracted in THF, an effect that in this solvent possibly overwhelms that of branching.

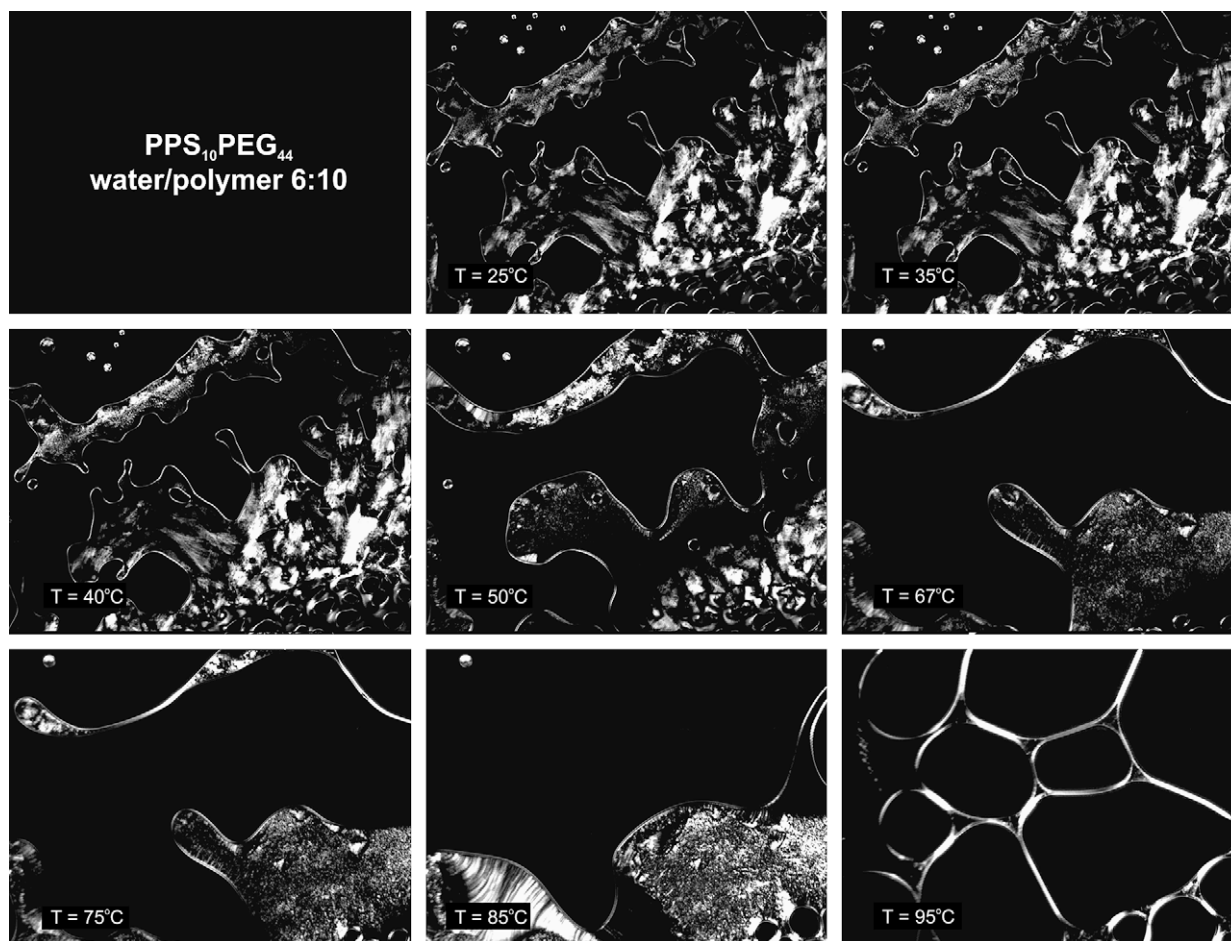


**Fig. 2.** Polarised Optical Microscopy pictures for the diblock copolymer Mono PPS<sub>10</sub>PEG<sub>44</sub> 62.5 wt.% in water as a function of temperature. The pictures initially focus on the edges of the lyotropic phase and no sample is present in the black areas. A first transition is apparent in the temperature range between 40 and 50 °C, with changes both in birefringence and in mobility of the phase: the edges become rounder and slowly rearrange to provide a smoother interface. At about 85 °C another phase transition takes place, yielding a yet birefringent material, characterised by very high fluidity. It is noteworthy that all samples were examined in a sealed environment to avoid water evaporation and ensure a constant water content.

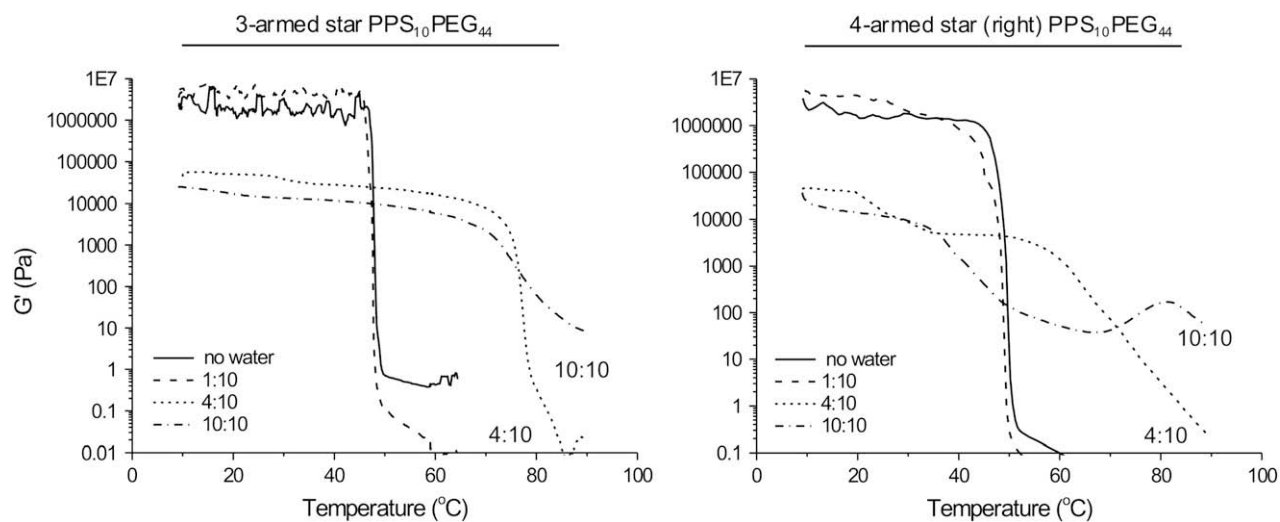


**Fig. 3.** Examples of dependence of the temperature dependence of the storage modulus ( $G'$ ) on the water content of the mixture for a tri-armed star (left) and a tetra-armed star (right) PPS<sub>10</sub>PEG<sub>44</sub>.

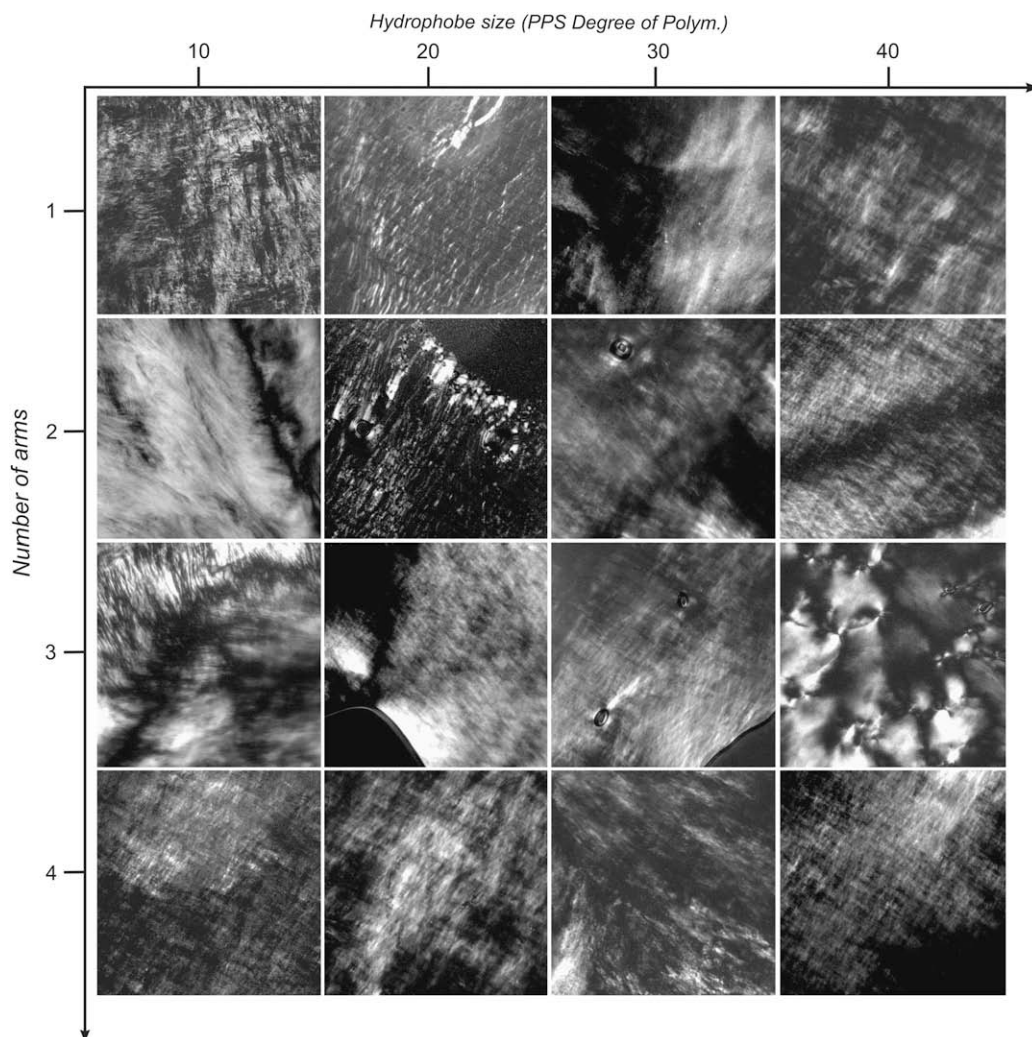


**Fig. 4.** POM pictures taken at constant water content (28 wt.%, i.e. 4:10 water/polymer) for all polymers synthesised in this study at a temperature of 65  $^{\circ}\text{C}$ .

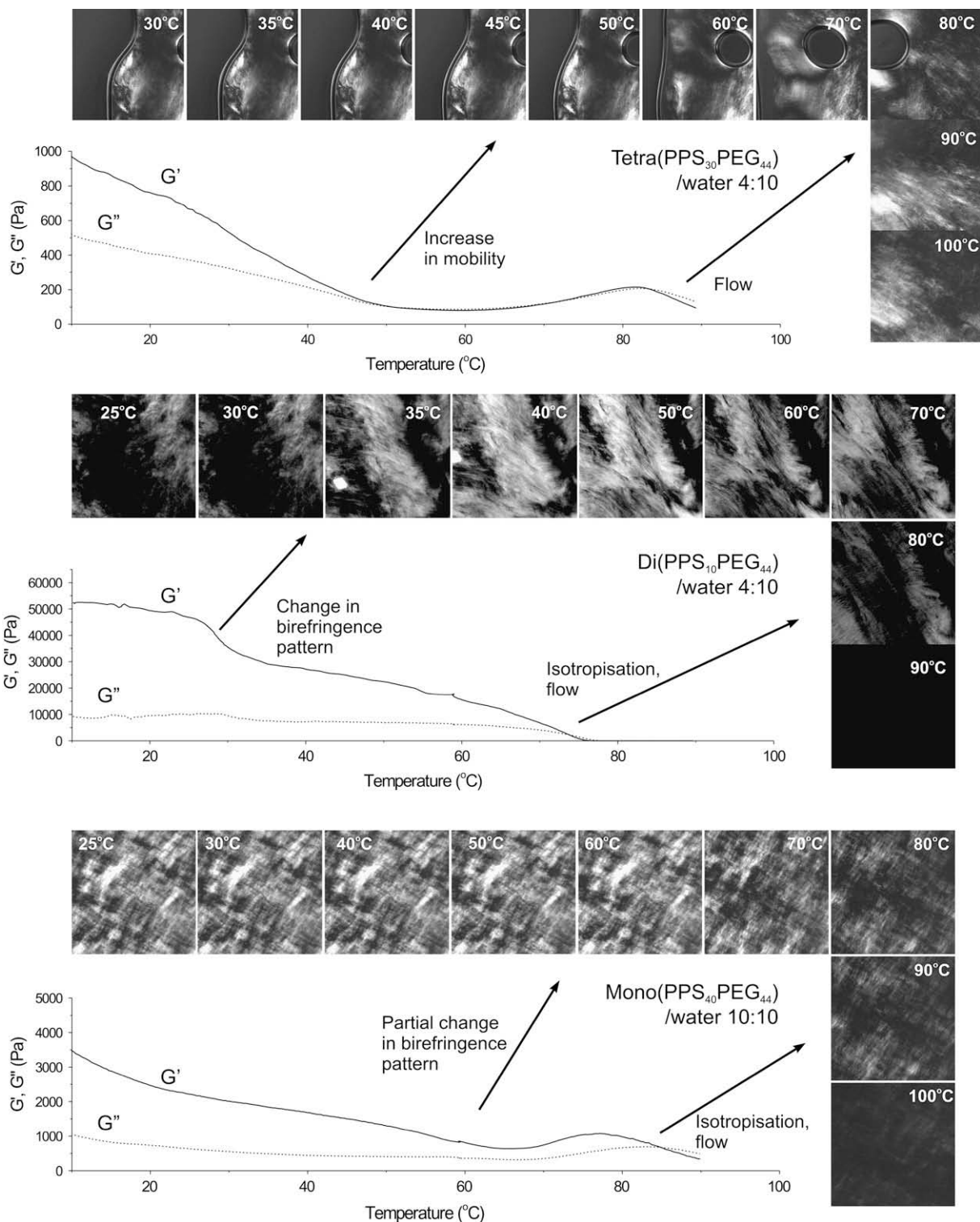


**Fig. 5.** Storage ( $G'$ ) and loss ( $G''$ ) moduli and POM pictures as a function of temperature for three representative polymer/water mixtures. *Bottom:* the diblock copolymer PPS<sub>40</sub>PEG<sub>44</sub> in a 50 wt.% water mixture shows a constant decrease in  $G'$  over the temperature range 20–65 °C;  $G'$  then plateaus and a corresponding change in birefringence is recorded. The birefringence pattern is then preserved without large variations until about 90 °C, when isotropisation takes place. *Middle:* the triblock copolymer PEG<sub>44</sub>PPS<sub>20</sub>PEG<sub>44</sub> (Di PPS<sub>10</sub>PEG<sub>44</sub>) in a 28 wt% water mixture exhibits a step change in  $G'$  at 27–30 °C, with a parallel drastic variation in birefringence; despite a continuous gradual decrease of  $G'$  the lyotropic phase does not show any visual change up to a temperature of 72–75 °C, where a gel–sol transition accompanied by isotropisation occurs. *Top:* the tetra-armed star Tetra PPS<sub>30</sub>PEG<sub>44</sub> polymer in a 28 wt% water mixture likely undergoes a first transition at 22–23 °C (change in  $G'$  slope); at higher temperatures (about 45 °C) the value of  $G'$  approaches that of  $G''$  and correspondingly the POM pictures reveal an increase in mobility (an entrapped air bubble starts moving). This fluid gel phase becomes a viscous liquid only above 80 °C, without, however, any apparent isotropisation.

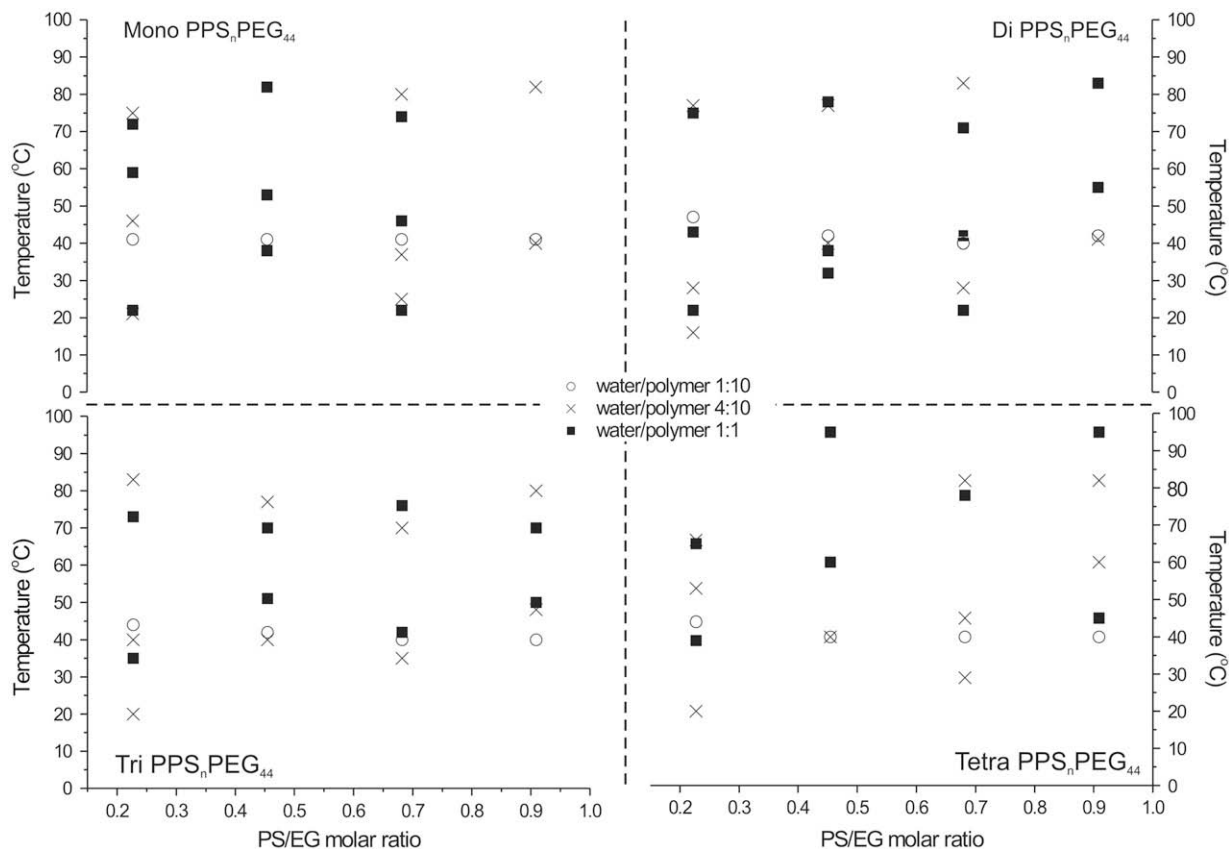


Fig. 6. Transition temperatures obtained from POM analysis and confirmed by shear rheometry (as steps in  $G'$  or changes in its slope), as a function of PPS/PEG weight ratio and degree of branching.

The absence of a branching-dependent coil contraction in very dilute solutions, however, is not necessarily an indication that in concentrated phases the presence of branching point has no influence on the PPS–PEG macromolecular organisation. We have therefore investigated possible differences in the lyotropic behaviour of this family of block copolymers.

### 3.1.1. Lyotropic aggregation

Being amphiphilic in nature, all PPS–PEG polymers provide associating behaviour in a water environment. In a number of reports the self-assembly of PPS–PEG diblock and PEG–PPS–PEG triblock copolymers was shown to lead to lyotropic (lamellar) phases at high concentrations, or to vesicular or micellar aggregates under high dilution [28,32].

Here we have focused on the influence of the macromolecular architecture on the lyotropic behaviour of concentrated PPS–PEG/water dispersions (water content  $\leq 50\%$ ), specifically focusing on qualitative differences in phase behaviour rather than on the precise characterisation of all phase diagrams for the 16 polymers synthesised.

As a general rule, all the polymers provided birefringent materials (Polarised Optical Microscopy, POM) at any water content between 0 and 50 wt.% at room temperature; the birefringence pattern and the mobility of the phases, however, strongly depended on temperature (Fig. 2).

Furthermore, all polymers, either pure or in water-containing mixtures, showed a predominantly elastic behaviour at room temperature, with  $G'$  values of a few MPa for the pure polymers or 9 wt.% water (1:10) mixtures, from 500 kPa to less than 1 kPa for mixtures with increasing water content (Fig. 3).

A sharp transition leading to a non-birefringent, low viscosity fluid was recorded for all pure polymers and their 9 wt.% water mixtures in between 35 and 45 °C (Fig. 3). We associate this transition to the melting of PEG blocks: although a linear PEG of similar molecular weights should exhibit a  $T_m \geq 55$  °C (both from experiments and from an easy extrapolation of literature data [33]), PEG spatial confinement in comb architectures [34] or in blocky structures with lamellar assembly [35] has been demonstrated to lower this value down to 35–42 °C, i.e. in the same range recorded in our experiments. It can be further observed that the presence of small amounts of water apparently had a negligible effect both on the mechanical properties of the materials and on the melting point of PEG.

High water content mixtures (28 wt.%, 50 wt.% or higher) presented a largely different temperature profile, with a much more gradual decrease of both  $G'$  (Fig. 3) and birefringence with increasing temperature.

Specifically, almost all samples

- exhibited a transition in the 35–45 °C temperature range, where a relatively small decrease in  $G'$  is accompanied by a change in the birefringence pattern and/or an increase in the mobility of the phase. These effects on mechanical properties and birefringence could not be associated to a simple PEG melting.
- showed a reasonably similar birefringence pattern in the 40–70 °C range, which we tentatively assigned to anisotropic lamellar structures (Fig. 4).
- presented a gel–sol transition ( $G''$  becoming larger than  $G'$ ), generally but not always accompanied by isotropisation, at temperatures comprised between 70 and 95 °C (Fig. 5).



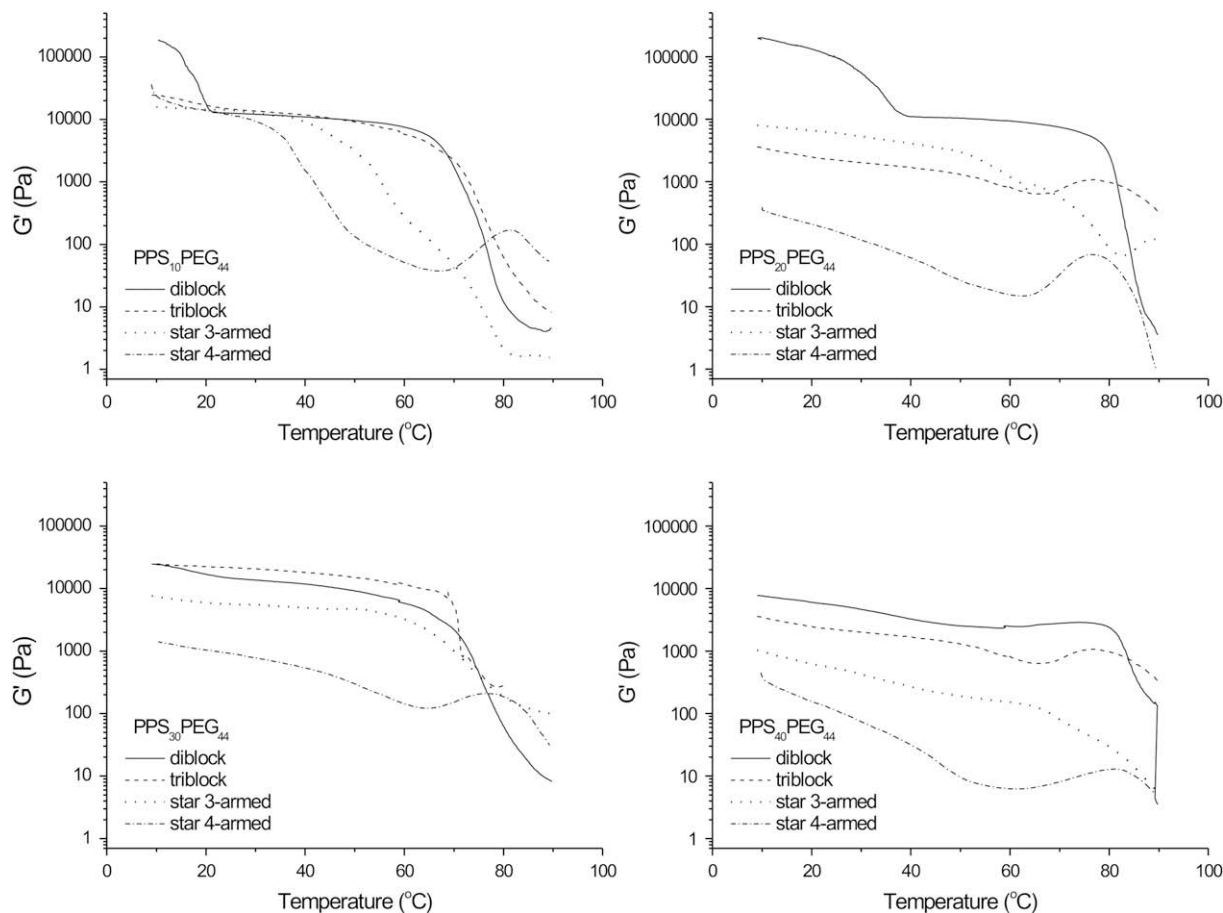


**Fig. 7.** Temperature dependence of the storage modulus ( $G'$ ) as a function of the PPS/PEG ratio and of the macromolecular architectures for 50 wt% polymer/water mixtures. Samples at 28 wt% water content showed a similar, although less pronounced, dependence on the branching (data not shown).

A plot of all transition temperatures observed through POM and confirmed by shear rheometry (Fig. 6) allows to better appreciate this relatively similar behaviour for all samples, which would therefore suggest that both the presence of a branching point in the hydrophobic block and the overall size of the hydrophobe play little influence on the phase behaviour.

However, a more careful comparison of the rheological data (Fig. 7) shows that the macromolecular architecture does influence the rheology of the material, with a marked decrease and a steeper temperature dependence for  $G'$  as a function of the branching degree. It is also noticeable that all the tetra-armed polymers and most tri-armed ones display a peculiar peak of  $G'$  at high temperatures, immediately below the isotropisation of the material; this peak is absent in most linear polymers, although present e.g. for the PPS<sub>40</sub>/PEG<sub>44</sub> diblock copolymer 10:10 in water (bottom graph in Fig. 3). On the other hand, the variation of PPS/PEG weight ratio between 0.38 and 1.5 (between 0.22 and 0.9 in terms of molar ratio of PS and EG repeating units) seems to produce no major effect, with the exception of the presence at low temperatures of a harder phase only for linear polymers with small hydrophobes (PPS<sub>10</sub>/PEG<sub>44</sub> building block).

From these results it is apparent that, within the PPS/PEG ratios considered, it is mostly the hydrophilic component (PEG) to determine the phase behaviour in water, therefore, it is reasonable to assume that the influence of branching on the lyotropic properties may be mediated by a branching-dependent organisation of the PEG chains.

In order to qualitatively confirm this hypothesis and highlight possible effects of macromolecular branching on PEG interfacial organisation, we have furthered the study by examining the behaviour of all amphiphilic polymers on water-supported monolayers.

### 3.1.2. Interfacial behaviour

Interfacial pressure/surface area isotherms were recorded for PPS-PEG block copolymers at the air-water interface on a Langmuir trough.

A first important issue to solve is whether, within the investigated PEG/PPS ratios, the interfacial area occupied by these polymers is

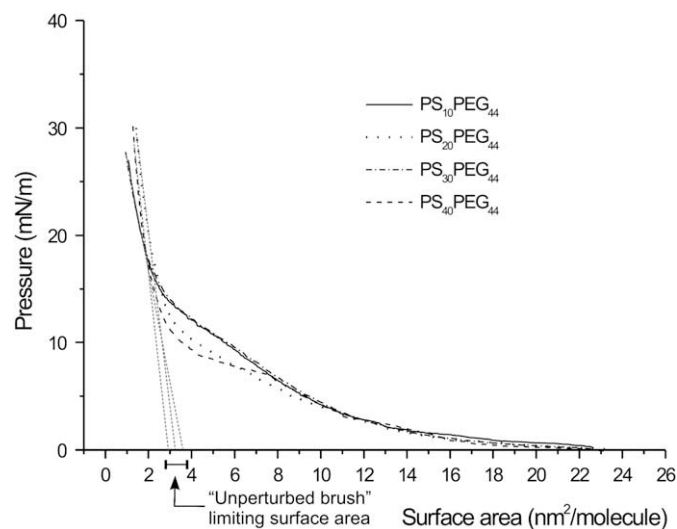


**Fig. 8.** Pressure/area isotherms obtained at the air-water interface in a Langmuir balance for a series of linear diblock copolymers with variable PPS/PEG ratio. An average “unperturbed” area of  $3.3 \pm 0.2$  nm<sup>2</sup>/molecule can be estimated.

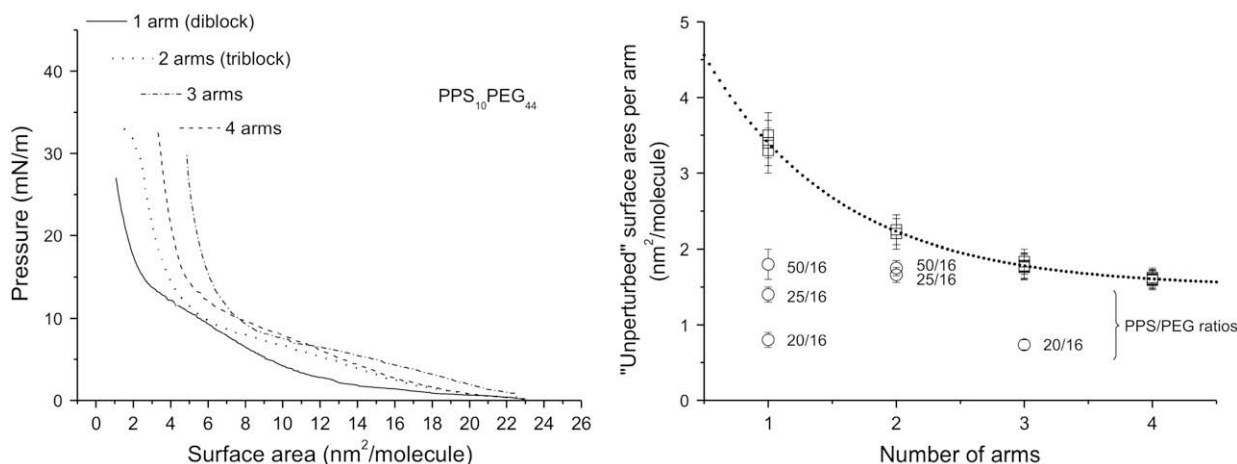


**Fig. 9.** Left: Pressure/area isotherms obtained at the air–water interface in a Langmuir balance for a series of polymers with variable branching degree and constant length and composition of each (PPS<sub>10</sub>PEG<sub>44</sub>). Right: the extrapolated “unperturbed” limit surface areas divided by the number of arms (surface areas per arm) for all the polymers prepared in this study (white squares) present the same value for all the polymers with the same number of arms and have an asymptotic behaviour. An exponential fit is presented as a guide for eyes. Other polymers with smaller PEGs and thus larger PPS/PEG ratios (white circles) on the contrary present little influence of branching.

mostly determined by the hydrophobic or the hydrophilic block, since this would allow to ascribe to one or the other phase any possible dependence of the surface area on branching. From previous investigations, mostly conducted on di- and triblock PPS<sub>n</sub>PEG<sub>16</sub> copolymers [28], we have concluded that the interfacial area of a PEG<sub>16</sub> would be matched by that of a PPS<sub>20–25</sub>; for polymers comprising PEG<sub>44</sub> and PPS < 60, as in our case, the surface area should therefore depend mostly on PEG. However, a number of MW-dependent factors, such as PEG hydrophilicity, may change this rule of thumb.

Assuming that the conformation of PPS at the air–water interface is not much different from that in a Q solvent, the PPS “unperturbed dimension” parameter  $A = \langle L_0^2 \rangle / M^{1/2}$ , where  $\langle L_0^2 \rangle$  is the square end-to-end distance under unperturbed conditions and  $M$  is the PPS molecular weight (please note that this parameter is related through the Flory universal constant  $F_0$  to the Mark–Houwink coefficient of the polymer under theta conditions, which is  $K_\theta = \Phi_0 \langle L_0^2 \rangle / M^{3/2}$ , which Nash and Pepper calculated to have a value  $A = 6–7 \times 10^{-2} \text{ nm mol}^{1/2} \text{ g}^{-1/2}$  for PPS [36]. From the well-known relationship between radius of gyration and mean end-to-end distance ( $\langle R_g^2 \rangle = \langle L^2 \rangle / 6$ ), a non-tethered PPS in random coil conformation would occupy an area  $\pi \langle R_g^2 \rangle = \pi \langle L^2 \rangle / 6 = \pi A^2 M / 6 \approx 0.16 N \text{ nm}^2$ , where  $N$  is the PPS degree of polymerisation and  $0.16 \text{ nm}^2$  is therefore an approximation of the surface area per PS monomeric unit. This is likely a gross overestimation of the real value and a far upper limit for PPS chains in amphiphilic structures, even more when they have a star morphology, which would determine a sound contraction of the coil [37]. Nevertheless, this value is still lower or at most analogous to the estimates of (coiled) PEG surface area per monomeric unit, which is reportedly comprised between  $0.28 \text{ nm}^2$  [19] for an extended and hydrated conformation and  $0.26 \text{ nm}^2$  for a folded and completely dehydrated one [38,39]. Since in the polymers studied here PEG’s degree of polymerisation (44) is always larger than PPS’ one (10–40), it can be expected that the PEG block would determine the overall macromolecular size at the hydrophobic/hydrophilic interface. Indeed, substantially identical Langmuir isotherms were recorded for polymers with the same branching degree, independently on the PPS/PEG ratios (Fig. 8).

Assuming the densely packed chains to behave as elastic springs (no entanglements), it is possible to extrapolate the area occupied by a single chain in the limit of complete surface occupation but no lateral pressure, i.e. an “unperturbed” limiting surface area of PEG in a conformation that is generally assumed to be quasi-brush [40],

although it is also suggested it to be a compact folded conformation [38].

It is noteworthy that a pseudo-plateau at low pressure is always present, evidence of an ubiquitous phase transition common to all high PEG content amphiphilic block copolymers [18,19], which is generally associated to its pancake-to-brush transition.

The comparison of polymers with constant PPS/PEG ratio and variable branching degree (Fig. 9, left) offers a very interesting point: the “unperturbed” limit surface area increased non-linearly with the number of arms of the polymer. Furthermore, considering the diblock structure as a single-arm architecture and the triblock as a 2-arm one, the “unperturbed” area per arm clearly decreased with increasing branching, asymptotically leading to a value of  $1.5 \text{ nm}^2/\text{arm}$ , while it was not influenced by the PPS/PEG ratio (Fig. 9, right). This very low asymptotic value could correspond to a very compact, possibly dehydrated, PEG chain in a quasi-brush or considerably folded conformation.

As a negative control, it can be seen that the limit areas for polymers with a lower PEG content, where PPS is assumed to determine the interfacial dimensions (Fig. 9, right, white circles; data in part from literature [28], in part from polymers prepared in other studies), showed a clear dependence on PPS molecular weight, but not on the degree of branching (for constant PPS/PEG ratios).

Therefore it can be concluded that (a) when the polymer interfacial area essentially depends on PEG (all the polymers prepared in this study), an increasing branching degree decreases the limit surface area per arm, and therefore the section of each PEG chain; at high branching this value appears to indicate much more compact (brush-like and possibly folded) PEG chains, (b) when the interfacial area depends on the hydrophobe, the influence of branching, if any, is overwhelmed by that of PPS size.

#### 4. Conclusions

We have prepared a library of amphiphilic PPS–PEG block copolymers, with constant PEG length and variable PPS length (10–40) and degree of branching (1–4 arms); in THF solution no clear influence of branching on hydrodynamic properties could be seen, most likely because PPS chains are in a collapsed state in that solvent. On the other hand, the behaviour in a water environment, showed both similarities and considerable differences as a function of branching and hydrophobic/hydrophilic ratio.

- The similarities between polymers with different hydrophobic/hydrophilic ratio and branching degree may stem from the fact that, throughout the library, the block copolymers' interfacial dimensions appeared to depend mostly on the hydrophilic block (which is constant), which would also mean the same sign of the interfacial curvature.
- The rheology of the lyotropic phases and the interfacial dimensions of the “unperturbed” polymers showed a clear dependence on the degree of branching, while the PPS/PEG ratio appears to have little or no effect in the range considered (which, again, is characterised by larger PEG than PPS). Specifically, PEG chains may adopt a more compact and less hydrated conformation with increasing branching; *inter alia*, this effect may change the nature of the interactions of PEG dandling with biomolecules, therefore, influencing the “stealth” character of PEGylated materials.

### Acknowledgements

Financial support from EPSRC (grant No. EP/C543564/1 and Advanced Research Fellowship for NT) is gratefully acknowledged.

### References

- [1] Torchilin VP. *Pharm Res* 2007;24(1):1–16.
- [2] Nardin C, Widmer J, Winterhalter M, Meier W. *Eur Phys J E* 2001;4(4):403–10.
- [3] Butun V, Liu S, Weaver JVM, Bories-Azeau X, Cai Y, Armes SP. *React Funct Polym* 2006;66(1):157–65.
- [4] York AW, Kirkland SE, McCormick CL. *Adv Drug Deliv Rev* 2008;60(9):1018–36.
- [5] Attwood D, Zhou ZY, Booth C. *Exp Opin Drug Deliv* 2007;4(5):533–46.
- [6] Discher DE, Ortiz V, Srinivas G, Klein ML, Kim Y, David CA, et al. *Prog Polym Sci* 2007;32(8–9):838–57.
- [7] Rijcken CJF, Soga O, Hennink WE, van Nostrum CF. *J Control Release* 2007;120(3):131–48.
- [8] Barner L, Davis TP, Stenzel MH, Barner-Kowollik C. *Macromol Rapid Commun* 2007;28(5):539–59.
- [9] Narrainen AP, Pascual S, Haddleton DM. *J Polym Sci Polym Chem* 2002;40(4):439–50.
- [10] Angot B, Taton D, Gnanou Y. *Macromolecules* 2000;33(15):5418–26.
- [11] Hedrick JL, Trollsas M, Hawker CJ, Atthoff B, Claesson H, Heise A, et al. *Macromolecules* 1998;31(25):8691–705.
- [12] Gitsov I, Frechet JM. *J Am Chem Soc* 1996;118(15):3785–6.
- [13] Saunders RS, Cohen RE, Wong SJ, Schrock RR. *Macromolecules* 1992;25(7):2055–7.
- [14] Pispas S, Hadjichristidis N, Potemkin I, Khokhlov A. *Macromolecules* 2000;33(5):1741–6.
- [15] Voulgaris D, Tsitsilianis C, Esselink FJ, Hadziioannou G. *Polymer* 1996;39:6429–39.
- [16] Wang L, Kilcher G, Tirelli N. *Macromol Biosci* 2007;7(8):987–98.
- [17] Ge ZS, Cai YL, Yin J, Zhu ZY, Rao JY, Liu SY. *Langmuir* 2007;23(3):1114–22.
- [18] Peleshanko S, Gunawidjaja R, Jeong J, Shevehenko VV, Tsukruk VV. *Langmuir* 2004;20(22):9423–7.
- [19] Gunawidjaja R, Peleshanko S, Genson KL, Tsitsilianis C, Tsukruk VV. *Langmuir* 2006;22(14):6168–76.
- [20] Peleshanko S, Tsukruk VV. *Prog Polym Sci* 2008;33(5):523–80.
- [21] Rehor A, Tirelli N, Hubbell JA. *Macromolecules* 2002;35(23):8688–93.
- [22] Napoli A, Valentini M, Tirelli N, Muller M, Hubbell JA. *Nat Mater* 2004;3(3):183–9.
- [23] Rehor A, Botterhuis NE, Hubbell JA, Sommerdijk N, Tirelli NJ. *Mater Chem* 2005;15(37):4006–9.
- [24] Rehor A, Hubbell JA, Tirelli N. *Langmuir* 2005;21(1):411–7.
- [25] Rehor A, Schmoekel H, Tirelli N, Hubbell JA. *Biomaterials* 2008;29(12):1958–66.
- [26] Khutoryanskiy VV, Tirelli N. *Pure Appl Chem* 2007;1703–18.
- [27] Napoli A, Tirelli N, Kilcher G, Hubbell JA. *Macromolecules* 2001;34(26):8913–7.
- [28] Napoli A, Tirelli N, Wehrli E, Hubbell JA. *Langmuir* 2002;18(22):8324–9.
- [29] Wang L, Kilcher G, Tirelli N. *Macromol Chem Phys* 2009;210(6):447–56.
- [30] Guven O. *Br Polym J* 1986;18(6):391–3.
- [31] Guaita M, Chiantore O, Burchard W. *Makromol Chem* 1991;192:2333–44.
- [32] Cerritelli S, Fontana A, Velluto D, Adrian M, Dubochet J, De Maria P, et al. *Macromolecules* 2005;38(18):7845–51.
- [33] Cheng SZD, Chen JH, Barley JS, Zhang AQ, Habenschuss A, Zschack PR. *Macromolecules* 1992;25(5):1453–60.
- [34] Bo G, Wesslen B, Wesslen KB. *J Polym Sci Polym Chem* 1992;30(9):1799–808.
- [35] Zhu L, Cheng SZD, Calhoun BH, Ge Q, Quirk RP, Thomas EL, et al. *Polymer* 2001;42(13):5829–39.
- [36] Nash DW, Pepper DC. *Polymer* 1975;16(2):105–9.
- [37] Birshtein TM, Zhulina EB. *Polymer* 1984;25(10):1453–61.
- [38] Cox JK, Yu K, Eisenberg A, Lennox RB. *PCCP Phys Chem Chem Phys* 1999;1(18):4417–21.
- [39] Shuler RL, Zisman WA. *J Phys Chem* 1970;74(7):1523–34.
- [40] daSilva A.M.G., Filipe E.J.M., dOliveira J.M.R., Martinho J.M.G., *Langmuir* 1996;12(26):6547–53.